

*Dedicated to Professor Liviu Literat
On the occasion of his 85th birthday*

INFLUENCE OF THE CITRIC ACID ON THE CERIUM SUBSTITUTED HYDROXYAPATITE MORPHOLOGY

ANA MARIA BARGAN^a, GABRIELA CIOBANU^{a,*},
CONSTANTIN LUCA^a, EUGEN HOROBA^a

ABSTRACT. In the present study the obtaining of the simple and substituted hydroxyapatite with cerium ions (Ce^{4+}) in presence of citric acid was studied. The hydroxyapatite samples were prepared by wet coprecipitation method. The structural properties of hydroxyapatite powders were characterized by scanning electron microscopy (SEM) coupled with X-ray analysis (EDX), X-ray powder diffraction (XRD) and Fourier Transform Infrared spectroscopy (FTIR). Like organic modifier, the citric acid has an influence on the morphology and particle size of hydroxyapatite as shown by XRD and SEM-EDX analysis. The results obtained indicated that cerium ions were incorporated into hydroxyapatite structure and the presence of citric acid was useful on the average crystallite size reduction of the samples obtained.

Keywords: *hydroxyapatite, citric acid, cerium*

INTRODUCTION

The bone mineral is described as a poorly crystalline non-stoichiometric apatite (biological apatite) with chemical composition of calcium phosphate [1]. Biological apatites are rarely stoichiometric, usually being calcium-deficient containing a wide variety of relatively small amounts of other substituted atoms. The major cause of nonstoichiometry is the incorporation of some impurities like cations or anions which may substitute calcium ions, phosphate and hydroxyl groups [2].

^a "Gheorghe Asachi" Technical University of Iasi, Faculty of Chemical Engineering and Environmental Protection, Prof. dr. docent Dimitrie Mangeron Rd., no. 73, 700050, Iasi, Romania. * Corresponding author: gciobanu03@yahoo.co.uk

The calcium phosphate group is a part of the bioceramics family being the most important inorganic hard tissues constituents of the bones and dentine material in the vertebrate species [3].

The calcium phosphates have been classified in to three major structural types [2,4]:

- 1) the apatite type $\text{Ca}_{10}(\text{PO}_4)_6\text{X}_2$ ($\text{X} = \text{OH}$ or F in hydroxyapatite or fluorapatite) and those related to apatite-type structures such as octacalcium phosphate (OCP) $\text{Ca}_8(\text{HPO}_4)_2(\text{PO}_4)_4 \cdot 5\text{H}_2\text{O}$ and tetracalcium phosphate (TTCP) $\text{Ca}_4(\text{PO}_4)_2\text{O}$;

- 2) the glaserite type which include polymorph forms of tricalcium phosphates (TCP) $\text{Ca}_3(\text{PO}_4)_2$ and

- 3) the CaPO_4 based compounds such as dicalcium phosphate dihydrate (DCPD) $\text{CaHPO}_4 \cdot 2\text{H}_2\text{O}$, dicalcium phosphate anhydrous (DCPA) CaHPO_4 and monocalcium phosphates $\text{Ca}(\text{H}_2\text{PO}_4)_2 \cdot \text{H}_2\text{O}$ and $\text{Ca}(\text{H}_2\text{PO}_4)_2$.

The synthetic hydroxyapatite, $\text{Ca}_{10}(\text{PO}_4)_6(\text{OH})_2$ (HA), is one of the most well-known phosphates that can be used in bone reconstruction for the implants fabrication with many biomedical applications. The hydroxyapatite bioceramics as bone substitute materials have more advantages such as: abundant supply, non-toxic, more biocompatible with an organism than other implanted materials and low cost. The hydroxyapatite is also being tested as an absorbent for organic molecules that exist inside the human body [5].

It is well known that the organic modifiers are used in the synthesis of the hydroxyapatite in order to control the morphology and size of the crystals [6]. Examples of such organic modifiers are: ethylene glycol, trisodium citrate, citric acid, polyethylene glycol, Tween20, D-sorbitol, sodium dodecyl sulphate, sodium dodecylbenzene sulphonate and polyoxyethylene [7].

In the past few years the scientists have been studied the substitution of the hydroxyapatite with rare earth elements and due to greater charge-to-volume ratios and despite their different valences, the Lanthanides readily displace calcium from biological apatite [8].

Discovered in 1803, cerium (^{58}Ce) is a trivalent atom although unique among the Lanthanides, it also has a quaternary valence (Ce^{4+}) [8]. Cerium is one of the cheapest and most abundant rare earths. However, high purity is usually required for its utilization in industry like sulphur control in steels, pyrophoric alloys, ceramic, catalyst support, polishing powders, phosphors luminescence, etc. [9].

The exchange of calcium ions in hydroxyapatite with cerium ions is an interesting subject in medical, catalysis and environmental sciences. In general, the compounds containing cerium ions have been used in medicine for a long time as antibacterial agents. Therefore, the incorporation of Ce ions into the hydroxyapatite lattice is important for the developing of artificial bones.

In this work we have studied the effect of citric acid like a chelating reagent during the precipitation process on the formation of simple and cerium substituted hydroxyapatite. The morphology and crystal structure of samples were characterized by SEM (scanning electron microscopy), EDX (Energy Dispersive X-ray spectroscopy), XRD (X-ray diffraction analyses) and FTIR (Fourier Transform Infrared spectroscopy) analyses.

RESULTS AND DISCUSSION

The properties of the hydroxyapatite can be improved by anion/cation substitutions in its network. Anion substitution reaction of PO_4^{3-} groups by HPO_4^{2-} and CO_3^{2-} and OH^- by F^- can modify the surface properties and the thermal stability of the material [10]. The substitution of Ca^{2+} with divalent cations (Sr^{2+} , Mg^{2+} , Cd^{2+} , Zn^{2+} , Pb^{2+} , Ba^{2+} , etc.) [11, 12, 13, 14], trivalent cations (Cr^{3+} , Al^{3+} and Fe^{3+}) and lately with rare earth cations [15], affects important characteristics of hydroxyapatite such as crystallinity, solubility, thermal stability, metabolizability, etc. [16].

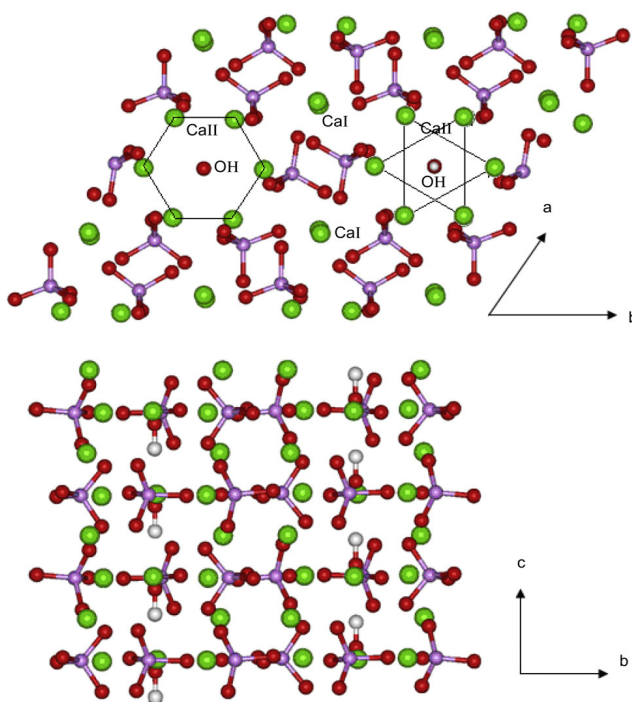


Figure 1. Representation of the hydroxyapatite structure perpendicular to the crystallographic c and a axes, showing the OH^- channels and the different types of Ca ions [18]

As illustrated in Figure 1, there are two crystallographically calcium sites in the hydroxyapatite unit cell: Ca (I) and Ca (II). Each Ca(I) is coordinated to nine O atoms belonging to six different PO_4^{3-} anions. The Ca(II) cations have a less regular seven-fold coordination: they are bound to six O atoms belonging to five different phosphates and to one hydroxyl group.

The incorporation of rare earth (lanthanide series) ions in the hydroxyapatite structure are favorable when there is a small difference in ionic radii which minimizes the difference in bond strength when one Ca^{2+} ion is substituted for another ion. Substitution in a crystal is expected to be common when there is an ionic radii difference of less than 15% [17]. With quite comparable dimensions, the Ce^{4+} ions (radius of 0.97 Å) can substitute Ca^{2+} ions (radius of 1.00 Å) during the synthesis process. The minimal difference (3%) in ionic radius between Ce^{4+} and Ca^{2+} contributes to the calcium replace.

In this research, in order to understand how the incorporation of a large cation like Ce^{4+} in the hydroxyapatite lattice and influence of citric acid can affect the cation and anion environment, the SEM, EDX, XRD and FTIR studies were carried out.

The SEM and EDX methods were performed in order to determine the surface elemental composition of the hydroxyapatite and cerium-substituted hydroxyapatite samples. Figure 2 shows the SEM micrographs of the calcinated samples. The samples without citric acid (HA and HA-Ce samples) consist of needle-like particles. Instead, the samples which content citric acid (HA-CitA and HA-CitA-Ce samples) consist of big aggregates of small particles due to the presence of calcium citrate complexes. These results indicate that citrate absorbs on the calcium phosphate nuclei, inhibits their growth and finally leading to the formation of a large number of small particles which contribute to a higher surface area, in agreement with literature data [19].

The EDX analysis (figures not shown) of the samples confirms the presence of the calcium, cerium, phosphorous, oxygen and carbon elements in certain proportions; no other elements are detected in the samples. The C signal in HA-CitA and HA-CitA-Ce samples is probably due to the traces of the uncalcined citric acid used as organic modifier in hydroxyapatite synthesis (due perhaps to the incomplete calcination of the samples). Using EDX method, the mass fractions of different elements in the hydroxyapatite and cerium-substituted hydroxyapatite samples were obtained and the atomic ratios were calculated, as presented in Table 1. The results confirm that cerium ions have been incorporated into the hydroxyapatite nanocrystals and the (Ce+Ca)/P atomic ratio in these powders is around 1.6.

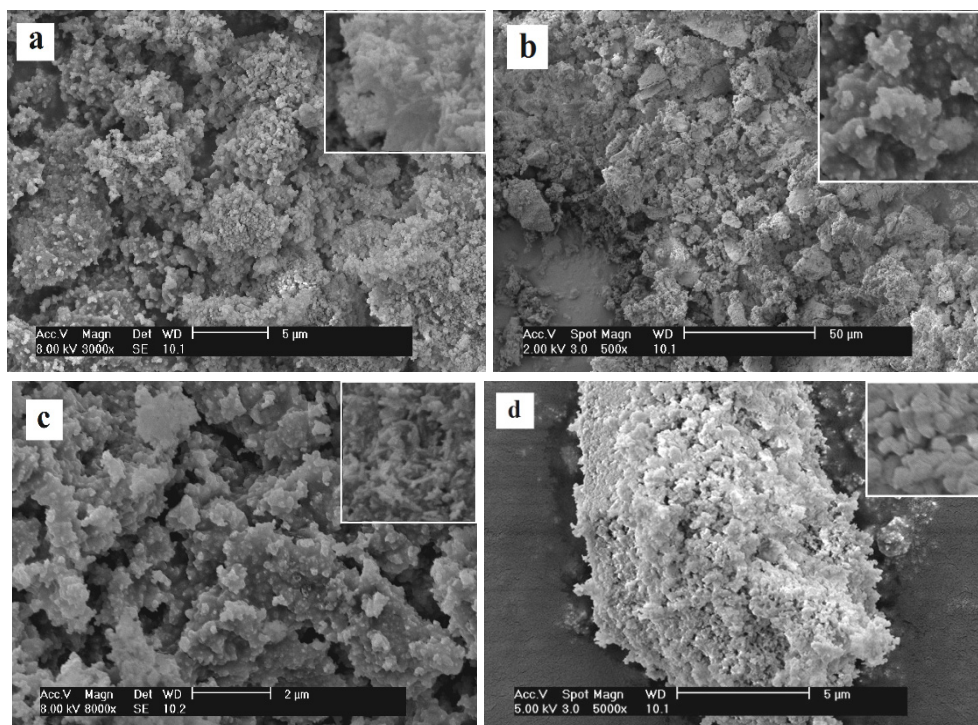


Figure 2. SEM images of the calcinated samples: (a) HA, (b) HA-CitA, (c) HA-Ce and (d) HA-CitA-Ce

Table 1. The elemental composition (% mass) and atomic ratio in the final products calcined in air at 850 °C

Sample	Ca (%)	P (%)	O (%)	C (%)	Ce (%)	(Ca+Ce)/P
HA	41.61	19.28	39.08	0	0	1.673
HA-Ce	40.5	19.91	32.08	0	7.51	1.660
HA-CitA	40.12	18.91	31.32	9.65	0	1.644
HA-CitA-Ce	39.07	18.98	29.32	5.35	7.28	1.680

The phase composition, lattice parameters, degree of crystallinity and size of the hydroxyapatite crystallites were determined by X-ray diffraction analysis. In the figure 3 it can see the patterns of the HA, HA-CitA and HA-CitA-Ce samples. All XRD patterns show the diffraction lines characteristic of hydroxyapatite, both present in standards and in literature. The major phase is hydroxyapatite which is confirmed by comparing data obtained with the JCPDS Data Card 09-0432 (for hydroxyapatite). The pattern of the sample

containing Ce (HA-CitA-Ce) exhibit similar but broader diffraction peaks, in agreement with a reduced degree of crystallinity of the cerium-substituted hydroxyapatite sample [15].

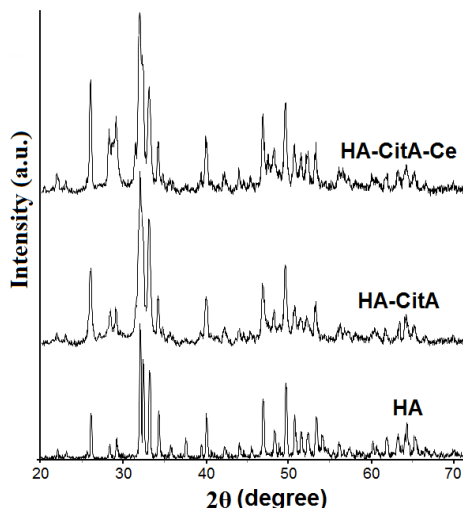


Figure 3. XRD patterns of the HA, HA-CitA and HA-CitA-Ce calcined samples

The average crystallite size (D) of the hydroxyapatite powders was calculated from XRD data using the Scherrer equation. The average crystallite size of the HA and HA-CitA hydroxyapatite powders were 59 and 54 nm, respectively. For the HA-Ce and HA-CitA-Ce cerium-substituted hydroxyapatite powders the average crystallite size were 47 and 43 nm, respectively. For samples doped with cerium, a small decrease in crystallite size was observed.

The FTIR spectra obtained from hydroxyapatite samples were given in Figure 4. The FTIR spectra of samples analysed provides information on the existing groups in the structure of hydroxyapatite, such as phosphate (PO_4^{3-}), hydroxyl (OH^-) and possibly carbonate (CO_3^{2-}) groups.

In Figure 4, the phosphate characteristic bands were observed at 472, 564, 602, 962, 1044, and 1092 cm^{-1} . These bands indicate the arrangement of the polyhedrons of PO_4^{3-} in the hydroxyapatite structure. The broader band between 3200 and 3500 cm^{-1} was produced by the water molecule adsorbed on the surface of hydroxyapatite and the stretching and vibration of O-H bonds on the surface of hydroxyapatite were located at 3590-3560 cm^{-1} . The entire FTIR spectrum shows the presence of an important peak in the range 1400-1500 cm^{-1} indicating the formation of calcium carbonate or calcium oxide in the apatite layer.

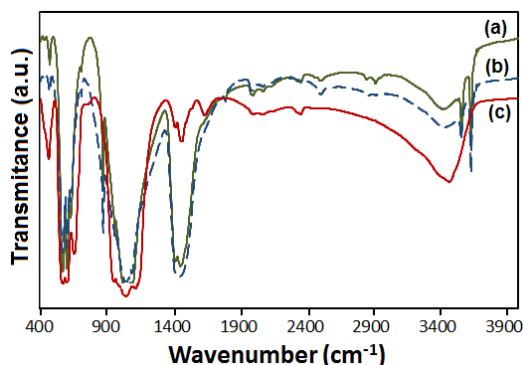


Figure 4. FTIR spectra of the calcined samples: (a) HA, (b) HA-CitA and (c) HA-CitA-Ce

The precipitation of calcium phosphate is inhibited in the presence of the citric acid, but in the small degree; this can be confirmed by the FTIR spectroscopy, in the figure 4, by the fact that the carboxyl group is identified in the spectra of sample HA-CitA at 1096 cm^{-1} for C-O stretch and at 2530 cm^{-1} and 2892 cm^{-1} for O-H bends. The intensity of the peaks is weak.

Compared to the spectrum of HA, no significant shift either to lower or higher wave number is observed upon doping with cerium ion. However, the intensity of all bands is weakened upon adding of Ce. The weakening of OH^- bands may be resulted from the breakage of balance of electric charge in hydroxyapatite; this is due perhaps to the substitution of Ca^{2+} with Ce^{4+} . In order to compensate these positive charges, OH^- may transform to O^{2-} , as suggested by Serret et al. [20]. The weakening of PO_4^{3-} bands may arise from the introduction of Ce^{4+} and subsequent alteration of the bonding force between ions, which lead to the weakening of the vibration of P-O and O-P-O.

EXPERIMENTAL SECTION

Hydroxyapatite powders can be synthesized by several methods, using a range of different reactants. The main processing techniques include wet chemical methods (precipitation), hydrothermal techniques, sol-gel methods, biomimetic deposition technique, electrodeposition [8], microemulsion [9] and spray drying method [10].

In this work hydroxyapatite simple and substituted with cerium ions were synthesized by coprecipitation method, as described elsewhere [21,22]. Reagent grade calcium hydroxide ($\text{Ca}(\text{OH})_2$), phosphoric acid (H_3PO_4), ceric sulphate pentahydrate ($\text{Ce}(\text{SO}_4)_2 \cdot 4\text{H}_2\text{O}$), citric acid ($\text{C}_6\text{H}_8\text{O}_7$) and sodium hydroxide (NaOH) used in this investigation were purchased from Sigma-Aldrich.

Calcium phosphate powders were prepared by neutralising a solution of $\text{Ca}(\text{OH})_2$ 0.01M with a solution of H_3PO_4 0.01M. We have made two solutions denoted A and B. The solution A (H_3PO_4 and distilled water) is added in the solution B ($\text{Ca}(\text{OH})_2$, $\text{C}_6\text{H}_8\text{O}_7$ and water) by dipping at 70°C and pH was adjusted at 11 with NaOH solution. The reaction was carried out at 70°C for 1 hour and then the slurry was aged for 48 h at room temperature, decanted and vacuum filtered. The obtained powder was dried at 110°C for 3 hours and calcined at 850°C during 3 hours.

For the cerium substituted hydroxyapatite preparation, $\text{Ce}(\text{SO}_4)_2$, $\text{Ca}(\text{OH})_2$ and $\text{C}_6\text{H}_8\text{O}_7$ were dissolved in water and then added to a solution of H_3PO_4 to attain the $(\text{Ca} + \text{Ce})/\text{P}$ mass ratio between 1,5 - 1,8. The pH was maintained at 10 - 11 with NaOH 10 M. The suspension was matured for 3 hours at approximately 70°C under magnetic stirring. After that, the powder was removed from the solution, washed with deionized water and dried at 60°C for 24 hours. The powder obtained was calcinated in an electrically heated furnace at a temperature of 850°C for 3 hours, in order to increase their crystallinity. In this study, all samples have denotes as follows: **HA** (simple hydroxyapatite), **HA-CitA** (hydroxyapatite with citric acid), **HA-Ce** (hydroxyapatite substituted with cerium) and **HA-CitA-Ce** (hydroxyapatite with citric acid and substituted with cerium).

The phase composition, crystal structure and morphology of the as obtained hydroxyapatite powders were analysed by scanning electron microscopy coupled with energy dispersive X-ray spectroscopy (SEM-EDX) (QUANTA 200 3D microscope), X-ray diffraction (XRD) (X'PERT PRO MRD diffractometer, using $\text{CuK}\alpha$ radiation $\lambda = 0.15418$ nm) and Fourier Transform Infrared spectroscopy (FTIR) (SPECTRUM BX II / PerkinElmer spectrophotometer).

CONCLUSIONS

The cerium-substituted hydroxyapatite powders were produced by coprecipitation reactions, using citric acid as organic modifier. The hydroxyapatite samples obtained have maintained the apatite structure. The Ce^{4+} ions were entered in the apatite crystal lattice by Ca^{2+} ions substitution. After substitution the crystallinity and the IR wave numbers of bonds in the HA-CitA-Ce sample decreased with the doping of cerium ion and the morphology of the nanoparticles changed from the rod-shaped (HA sample) to the needle-shaped (HA-Ce sample). The XRD pattern of the HA and HA-CitA samples display well-defined and sharp peaks in agreement with a high degree of crystallinity, with no visible modifications. The pattern of the sample containing Ce (HA-CitA-Ce) exhibit broader diffraction peaks, in agreement with a reduced degree of crystallinity of the cerium-substituted hydroxyapatite sample. The results obtained indicated that cerium ions were incorporated into hydroxyapatite structure and the presence of citric acid was useful on the average crystallite size reduction of the samples obtained.

REFERENCES

1. H. Yuan, K. de Groot, *Learning from Nature How to Design New Implantable Biomaterials*, **2004**, 37-57.
2. M. Mathew, S. Takagi, *Journal of Research of NIST*, **2001**, 106, 1035.
3. S. Pramanik, A.K. Agarwal, K.N. Rai, A. Garg, *Ceramics International*, **2007**, 33, 419.
4. W.J.E.M. Habraken, J.G.C. Wolke, J.A. Jansen, *Advanced Drug Delivery Reviews*, **2007**, 59, 234.
5. M. Jarcho, *Clinical Orthopedics and Related Research*, **1981**, 157, 259.
6. D.N. Misra, *Journal of Dental Research*, **1996**, 75, 1418.
7. A. Wang, H. Yin, D. Liu, H. Wu, Y. Wada, M. Ren, Y. Xu, T. Jiang, X. Cheng, *Materials Science and Engineering: C*, **2007**, 27(4), 865.
8. J.P. Garner, P.S.J. Heppell, *Burns*, **2005**, 31, 539.
9. Ş. Sert, C. Kütahyalı, S. İnan, Z. Talip, B. Çetinkaya, M. Eral, *Hydrometallurgy*, **2008**, 90, 13.
10. S. Shimoda, T. Aoba, E. Morenoe, Y. Miake, *Journal of Dental Research*, **1990**, 69, 173.
11. M.D. O'Donnell, Y. Fredholm, A. De Rouffignac, R.G. Hill, *Acta Biomaterialia*, **2008**, 4(5), 1455.
12. G. Qi, S. Zhang, K.A. Khor, S.W. Lye, X. Zeng, W. Weng, C. Liu, S.S. Venkatraman, L.L. Ma, *Applied Surface Science*, **2008**, 255, 304.
13. T. Tamm, M. Peld, *Journal of Solid State Chemistry*, **2006**, 179, 1581.
14. A. Yasukawa, K. Gotoh, H. Tanaka, K. Kandori, *Colloids and Surfaces A: Physico-chemical and Engineering Aspects*, **2012**, 393, 53.
15. Z. Feng, Y. Liao, M. Ye, *Journal of Materials Science: Materials in Medicine*, **2005**, 16, 417.
16. N.S. Resende, M. Nele, V.M.M. Salim, *Thermochimica Acta*, **2006**, 451, 16.
17. R.D. Shannon, *Acta Crystallographica*, **1976**, A32, 751.
18. D. Laurencin, N. Almora-Barrios, N.H. de Leeuw, C. Gervais, C. Bonhomme, F. Mauri, W. Chrzanowski, J.C. Knowles, R.J. Newport, A. Wong, Z. Gan, M.E. Smith, *Biomaterials*, **2011**, 32, 1826.
19. K.S. Tenhuisen, P.W. Brown, *Journal of Materials Science: Materials in Medicine*, **1994**, 5, 291.
20. A. Serret, M.V. Cabanas, M. Vallet-Regi, *Chemistry of Materials*, **2000**, 12, 3836.
21. G. Ciobanu, D. Ignat, G. Carja, C. Luca, *Environmental Engineering and Management Journal*, **2009**, 8, 1347.
22. G. Ciobanu, S. Ilisei, M. Harja, C. Luca, *Science of Advanced Materials*, **2013**, 5(8), 1090.